Chemical Physics Letters 754 (2020) 137707

Contents lists available at ScienceDirect

Chemical Physics Letters

journal homepage: www.elsevier.com/locate/cplett

Research paper

A theoretical investigation of different point charges combined with GAFF and OPLS-AA for acetic anhydride

Veerapandian Ponnuchamy*

InnoRenew CoE, Livade 6, 6310 Izola, Slovenia
University of Primorska, Andrej Marušič Institute, Titov trg 4, 6000 Koper, Slovenia

HIGHLIGHTS

- Different point charges were obtained from DFT calculations for acetic anhydride.
- RESP2, AM1-BCC and CM5 charges were fitted.
- GAFF and OPLS potentials were applied with fitted charges for bulk simulations.
- The simulated density and viscosity values were in good agreement with experiments.

ARTICLE INFO

Keywords:
Acetic anhydride
Point charges
RESP2
AM1-BCC
CM1
CM5
Quantum chemistry
Molecular dynamics
Density
Viscosity

ABSTRACT

Four different charge methods such as RESP2, AM1-BCC, CM1 and CM5 were employed to investigate the properties of acetic anhydride in a bulk phase simulation with GAFF and OPLS force field potentials. These charges were obtained from quantum mechanical calculations by fitting electrostatic potential for RESP2, AM1-BCC and Hirshfeld population for CM5 charges. The calculated density and viscosity values from molecular dynamics simulation were in good agreement with experimental values; however, GAFF with RESP2/AM1-BCC models exhibited higher error (2.1–3.07%) than OPLS with CM1/CM5, which showed the error around 0.1–0.5%.

1. Introduction

Acetic anhydride has been widely used for acetylation of a large variety of compounds that include acetylation of wood to protect it from microbiological attack, conversion of alcohols into esters, radio labelling of proteins and blocking metal cluster growth [1–7]. Furthermore, acetylated compounds such as cellulose acetate, acetylated starch, acetylated glycerol and acetylated salicylic acid are used for photographic films, membranes, fibers, food applications, cryogenics, plastic/fuel additives and production of aspirin [8–13]. Acetic anhydride is anhydride of acetic acid, exists as colorless liquid with a sharp odor and highly corrosive, and it was first synthesized by Charles Frédéric Gerhardt in 1852. Although it has been used extensively for acetylating agent in numerous applications, many countries have banned it because of handling for the production of heroin and improvised explosive devices (IED) [14–16]. However, physico-chemical properties of acetic anhydride at atomic or molecular level is yet unknown. Therefore, understanding acetic acid anhydride at molecular level is more important to analyse in the bulk liquid phase to study and use for different applications.

In general, GAFF and OPLS all-atom force fields are commonly used for molecular dynamics simulations to describe a wide range of organic molecules [17,18]. Electrostatic interaction is more important in the force fields and can be accounted through atom-centered partial charges. These partial charges have been derived with the help of various methods such as restrained electrostatic potential (RESP), AM1-BCC, charge models (CMs), Chelpg and implicitly polarized charge method (IPolQ) [19–26]. These methods can be applied for different organic systems of interest. However, RESP and AM1-BCC methods are the most predominant methods used for a majority of cases to fit partial charges for coulombic interaction in the force field. Between the two methods, RESP is more expensive than the later and HF/6-31g* level is

* Address: InnoRenew CoE, Livade 6, 6310 Izola, Slovenia.
E-mail address: veerapandian.ponnuchamy@innorenew.eu.

https://doi.org/10.1016/j.cplett.2020.137707
Received 15 May 2020; Received in revised form 3 June 2020; Accepted 9 June 2020
Available online 10 June 2020
0009-2614/ © 2020 Elsevier B.V. All rights reserved.

used as default. It is stressed that the charges obtained from a lower level, for instance, HF/6-31g*, lead to erroneous estimation of absolute free energies of hydration. Therefore, high-level quantum chemical (QC) density functional theory (DFT) calculations should be required to compute ESP for obtaining accurate charges and eventually used for accurate simulations. Recently, the authors have reported a new method called RESP2 that takes into account the contribution from both gas- and aqueous-phase calculation, and several higher level DFT functionals and basis sets were employed for QC calculations [27]. This particular method overcomes the issues with RESP method as approximately described self-polarization of molecules in condensed phase. CM charges [24,28] combined with OPLS force field have been used, and they can be mapped from Hirshfeld population analysis [29]. Although CM method exquisitely provides results for gas-phase dipole moments, their adequacy in condensed phased simulation remains doubtful. Therefore, recent studies have evaluated CM approaches and stated that a scaling factor is essential to ensure the simulations performed in condensed phases and the appropriate scaling factor 1.14 for CM1 and 1.27 for CM5 were considered [23,24].

The present study focuses on the evaluation of point charges for acetic anhydride molecule using quantum chemical calculations. RESP2, AM1-BCC and CM5 charges have been extracted with different DFT functionals and basis level of theory. Apparently, the obtained point charges will be used to perform MD simulations using two different potentials – GAFF and OPLS. Density and viscosity are mainly focused in this study due to available experimental data found in the literature for acetic anhydride. Thus, the simulated density and viscosity are compared with experiments to validate the charges. To the best our knowledge, this is the first study to propose the charges for force field based molecular dynamics (MD) simulations and validate with experimental values for the case of acetic anhydride.

2. Computational details

2.1. Density functional theory (DFT) calculations

DFT calculations have been employed to optimize isolated acetic anhydride molecule using GAMESS-US package [30]. There are three different DFT calculations performed in order to extract the appropriate charges such as RESP1, AM1-BCC and CM5 by fitting electrostatic potential (ESP) and Hirshfeld population for GAFF and OPLS potentials:

(1) *RESP2*: Hybrid meta GGA functional TPSSh [31] with cc-pV(D + d)Z [32] basis has been chosen for RESP2 charges calculations. As stated in the reference, the authors [27] have used PW6B95/cc-pV(D + d)Z level of theory in both vacuo and implicit solvent (ε = 78.39) to generate RESP2 charges. It should be pointed out that a similar type of hybrid meta TPSSh functional was considered in this study due to absence of PW6B95 functional in the GAMESS-US package at the time of the study. This TPSSh functional was successfully used recently to predict the partial charges for organic molecules and tested in MD simulations [33]. Both gas- and aqueous-phase (with water using PCM method) calculations were carried-out to extract the ESP using Molden [34], and then two-stage fitting was performed according to the Mertz–Kollman scheme [35] implemented in Multiwfn [36]. The resulting two charge sets were combined with a mixing parameter δ in this equation,

$$q_i^{RESP2} = (1 - \delta) q_i^{gas} + \delta q_i^{aqueous} \quad (1)$$

In the above equation, δ describes the polarity of the RESP2 charge; for instance, if $\delta = 0$, the calculated RESP2 charges are less-polar or gas-phase and when $\delta = 1$ it represents that the RESP2 charges are higher polar aqueous phase charges. The most optimal value for δ was chosen as 0.6 (60% contribution from aqueous and 40% from gas phase), like in the reference[27], to describe accurately the atom-centered partial charges.

(2) *AM1-BCC*: This type of atomic point charges has been emulated at HF/6-31 g(d) electrostatic potential. The isolated geometry of acetic anhydride was optimized, and charges were determined using Amber's Antechamber module[37].

(3) *CM5*: In this case, M06-L functional with MG3S basis set [38] was used for gas-phase CM5 charge extraction, and this particular level of theory yields atomic charges that are successfully used with OPLS for MD simulations [28]. CM5 charges were mapped with help from a fitting program implemented in Multiwfn package. A scaling factor of 1.27 was adopted with obtained CM5 partial charge to assure condensed phase MD simulations.

2.2. Molecular dynamics (MD) simulations

MD simulations were performed using LAMMPS [39] packages for acetic anhydride system, containing 1000 molecules in total to ensure no size effects could be possible. Standard 12-6 Lennard-Jones and Coulombic interaction were considered to model intermolecular interactions. The most common force fields such as the generalized Amber force field [17] (GAFF) and OPLS [18] were taken into account for LJ parameters. The different atomic charges, RESP2/AM1-BCC and CM5 combined with pre-existing GAFF and OPLS parameters are illustrated in Table 1 and atom labelling is presented in Fig. 1. It is mentioned here that CM1 charges were also considered in this study to evaluate the properties of acetic anhydride with OPLS potential and compared with other charge methods. These CM1 charges can be extracted from LigParGen web server [40] in which the charges are scaled 1.14*CM1 [24].

Four different MD simulations were conducted with respect to point charges, two as each simulation of GAFF with RESP2 and AM1-BCC, and the other two simulations as CM1 and CM5 with OPLS. Initial

Table 1
Force field parameters used in this study with different charge models for acetic anhydride. The LJ parameters, ε and σ values are given in kcal/mol and Å, respectively.

Atom	GAFF				OPLS			
	ε	σ	q_{RESP2}	$q_{AM1\text{-}BCC}$	ε	σ	$q_{1.27*CM5}$	$q_{1.14*CM1}$ [a]
H1	0.0157	2.65	0.1543	0.0784	0.0300	2.50	0.1343	0.1307
C1	0.1094	3.40	−0.4911	−0.1520	0.0660	3.50	−0.2731	−0.2644
C2	0.0860	3.40	0.7438	0.6540	0.1050	3.75	0.3580	0.4727
O1	0.2100	2.96	−0.4763	−0.4810	0.2100	2.96	−0.3650	−0.3800
OE	0.1700	3.00	−0.4785	−0.5124	0.1400	2.90	−0.2456	−0.4421
O2	0.2100	2.96	−0.4762	−0.4810	0.2100	2.96	−0.3650	−0.3796
C3	0.0860	3.40	0.7433	0.6540	0.1050	3.75	0.3580	0.4734
C4	0.1094	3.40	−0.4902	−0.1520	0.0660	3.50	−0.2731	−0.2648
H2	0.0157	2.65	0.1541	0.0784	0.0300	2.50	0.1343	0.1309

[a] Scaled 1.14*CM1 charges were extracted from LigParGen web server [40].

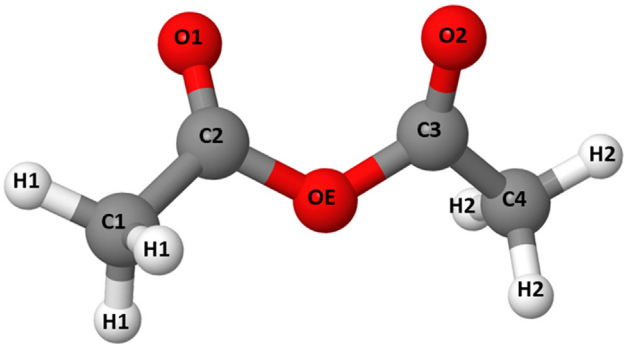

Fig. 1. Atom labelling for acetic anhydride molecule.

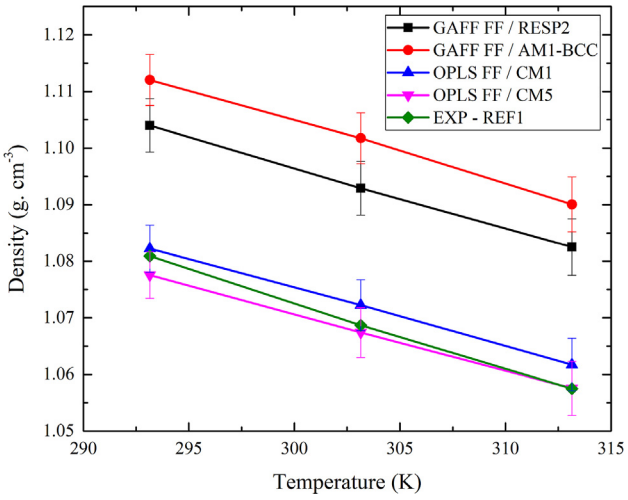

Fig. 2. The simulated density (in g·cm^{-3}) of acetic anhydride at different temperature (K) using different charge models and compared with experiment [43].

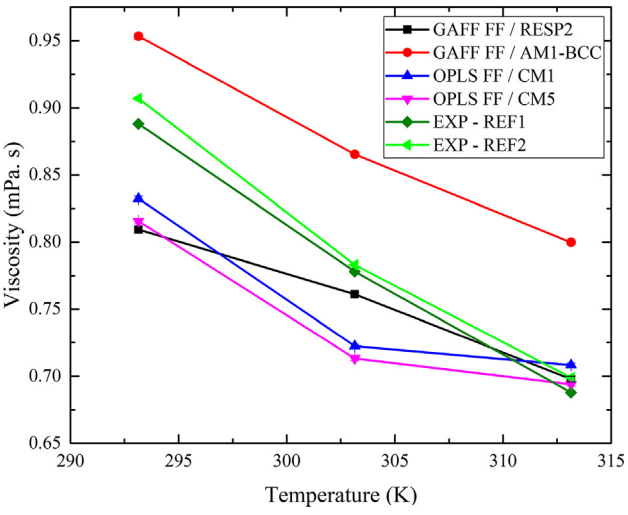

Fig. 3. Bulk viscosity as a function of temperature for a bulk acetic anhydride system, computed using GAFF (RESP2/AM1-BCC) and OPLS (CM1/CM5) and compared with experimental values that can be found in Reference [43].

configuration of simulation box contained 1000 acetic anhydride molecules packed using Packmol [41] and moltemplate tool available in LAMMPS. Each system starts with minimization, followed by NPT simulation for 2 ns to get the correct density. After that, NVT ensemble simulations were performed to extract the viscosity of the liquid using Green-Kubo method (Equation (2)). All simulations were performed with the integration step of 1 fs at 293.13 K, 303.15 K and 313.15 K to compare experimental data. The cut-off distance of 10.0 Å for both LJ and Coulomb potentials was considered and Particle Mesh Ewald method was employed for electrostatic interactions.

The viscosity of the bulk acetic anhydride was calculated using the ensemble average of the autocorrelation function of pressure tensors at constant temperature and volume. The Green-Kubo relationship [42] is widely used to calculate the shear viscosity of the liquids, which is expressed as,

$$\eta = \frac{V}{k_B T}\int_0^\infty \langle P_{ij}(t)\cdot P_{ij}(0)\rangle dt \quad (2)$$

where V represents the total volume of the simulation box, k_B is the Boltzmann constant, T is temperature and P_{ij} represents the pressure tensor of the system. In our case, only off-diagonal pressures (P_{xy}, P_{yz} and P_{xz}) were considered to evaluate the viscosity and angle brackets denote ensemble average. Each pressure tensor was autocorrelated every 3 fs during simulations and the final viscosity value was calculated by considering final 5 ns from 10 ns of total trajectory simulation window.

3. Results and discussion

3.1. Density

Bulk density provides a clear insight about the molecule-level interaction and arrangement of acetic anhydride at macroscopic level. A detailed experimental analysis was performed for acetic anhydride at different temperature. The reported experimental density in the reference [43] and therein is 1.08089 g·cm^{-3} at 298.15 K, and at higher temperature 303.15 K and 313.15 K, the densities were found to be 1.06871 g·cm^{-3} and 1.0565 g·cm^{-3}, respectively. Comparison of experimental density with calculated MD densities with different potentials are presented in Fig. 2. It is clearly seen from Fig. 2 that both GAFF and OPLS potentials with different charge models predicted densities that were in consistent agreement to the experimental values at 293.15 K. Among the investigated charge model in the case of OPLS, the value associated with CM1 charge model is close to the experimental value with an error of around 0.12%, whereas it was about 0.3% for CM5. The difference in error values between CM1 and CM5 is almost negligible and both charge methods can be used for acetic anhydride simulations. It is interesting to note that GAFF exhibited slightly higher density, about 0.3 g cm^{-3}, than OPLS methods and apparent error is about 2.13% with RESP2 and 2.8% with AM1-BCC to the experimental values. At higher temperature, the bulk density values of acetic anhydride in all cases decreases and the difference can be seen in Fig. 2. It seems that GAFF potential exhibits a similar trend in error at even higher temperature for RESP2 and AM1-BCC, whereas in the case of OPLS/CM1, it shows a bit higher error but still the error in under 0.5%. OPLS/CM5 model provides a consistent density at 313.15 K and the calculated error is 0.1%. Although the overall trend for GAFF potential with RESP2/AM1-BCC is consistent with experimental trend, a little deviation occurred as compared to OPLS. This is due to the fact that OPLS/AA potential was extensively developed for organic liquids, whereas GAFF potential development was not mainly focused for liquids. Our obtained results were consistent to the Reference[44].

3.2. Viscosity

The experimental viscosities for pure acetic anhydride can be found in reference [43] and therein. The reported values are found to be 0.888/0.907, 0.778/0.783 and 0.688/0.699 mPa. S at 293.15, 303.15 and 313.15 K, respectively. The calculated viscosity values from MD simulations together with experimental values are plotted in Fig. 3. A clear trend has been observed between experimental and calculated viscosities (in Fig. 3) based on different potentials with different

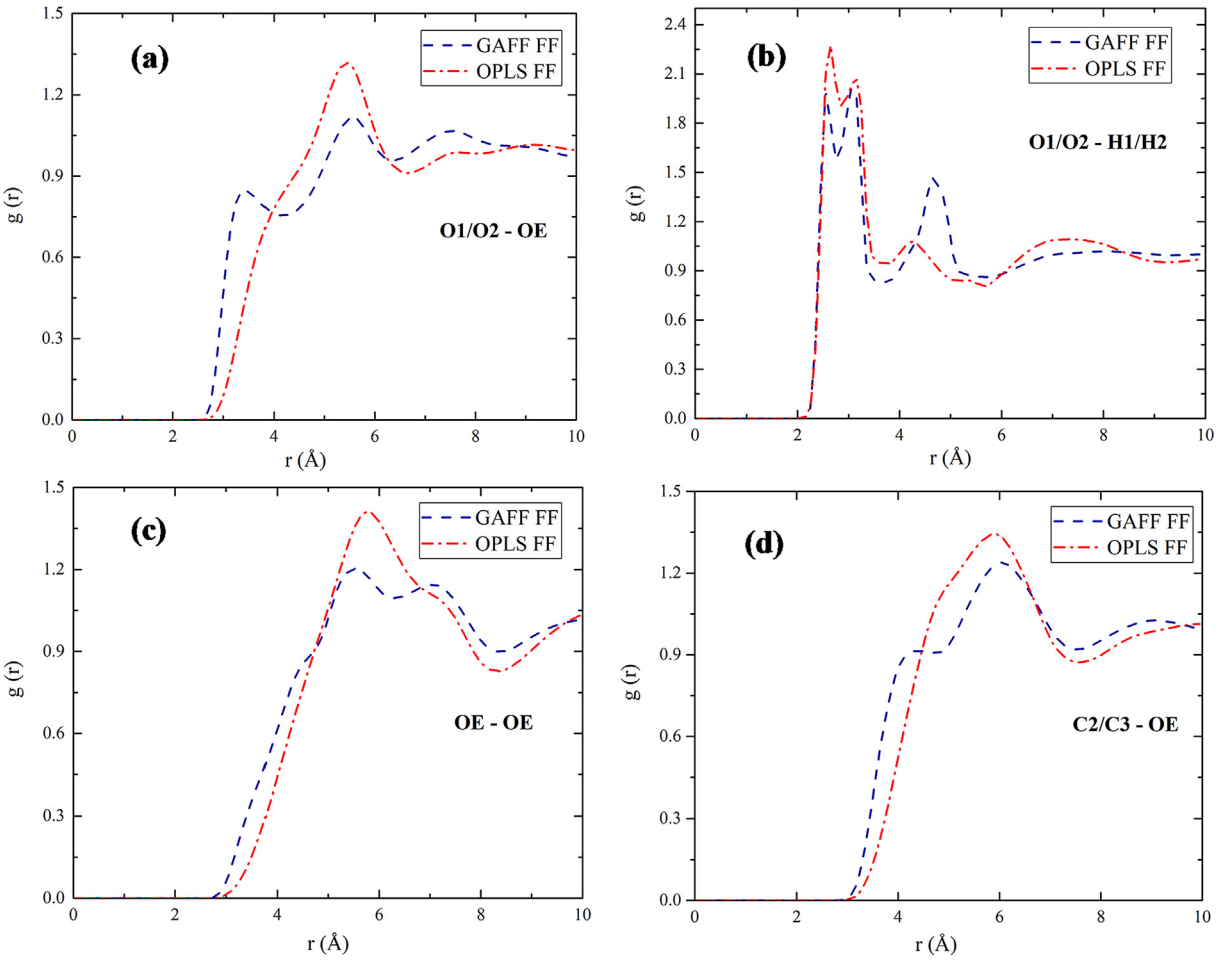

Fig. 4. Atom-atom radial distribution functions calculated for pure acetic anhydride system at 293.15 K and compared between GAFF (RESP2) and OPLS (CM1) for (a) carbonyl oxygen (O1/O2) – ester oxygen (OE), (b) carbonyl oxygen (O1/O2) – methyl group hydrogens (H1/H2), (c) ester oxygen (OE) – ester oxygen (OE) and (d) methyl carbon (C2/C3) – ester oxygen (OE); See Fig. 1. For atom labelling.

charges. Among the charge methods employed, both OPLS/CM1 and OPLS/CM5 methods exhibit a good correlation with experimental values followed by GAFF potential method at 293.15 K. The error was found to be less than 8.0% in the case of OPLS potentials with literature values; however, it was estimated at about 9.6% for the case of GAFF with RESP2. It is interesting to see that GAFF/AM1-BCC exhibits a good correlation with experiments at 293.15 K with an error of 6.8%. Although GAFF/RESP2 method provides lower viscosity compared to OPLS methods, it should be noted that at higher temperatures, for instance, 303.15 and 313.15 K, this method indeed gives viscosities that are in close agreement with experimental findings. Higher deviation occurred for GAFF/AM1-BCC at increasing temperature. However, the error between values is negligible between different methods and experiments, and all the investigated potential can be used for extensive analysis of acetic anhydride solution with molecular dynamics simulations.

3.3. Radial distribution function

Intermolecular site-site interaction between molecules can be calculated through radial distribution function (RDF). RDFs provide a clear description of local molecular ordering in the bulk system and also analyze its arrangements. Although acetic anhydride molecule is polar, it is evident that acetic anhydride molecules have weak intermolecular interaction due to lack of strong hydrogen bonding donor in the molecule. However, it makes a strong interaction through hydrogen bonds with other solvents that have a hydrogen bond donor, for instance, acetic acid and water.

Some of the RDFs of liquid acetic anhydride using GAFF and OPLS potentials are illustrated in Fig. 4. Although two different charges were investigated in the case of OPLS potential, no significant changes in RDFs were observed between CM1 and CM5; therefore, OPLS CM1 model was considered for the comparison. Similarly, in the case of GAFF, RESP2 trajectory was used for RDF analysis. All simulated RDFs indicate that two investigated potentials show almost similar trend, except for the case of carbonyl oxygen O1/O2 with ester OE (in Fig. 4a) where two maxima were observed at 3.45 Å and 5.55 Å with GAFF. Although acetic anhydride does not have hydrogen donor, Fig. 4b suggests the abundance of RDFs of carbonyl oxygens O1/O2 with methyl hydrogen H1/H2 and the typical distance were found to be 2.55 Å and 2.65 Å in the case of GAFF and OPLS potentials, respectively. A pronounced peak in the range of 5.4–5.8 Å in the case of ester oxygen – ester oxygen RDF is shown in Fig. 4c. The long-distance interaction for OE-OE revealed that ester oxygen atoms were hindered during the simulation because of carbonyl and methyl groups in acetic anhydride. Similar behavior was also predominant for methyl carbon and ester oxygen. Comparing the obtained RDF structural results from two potentials, both potentials show almost similar behavior in the simulation of acetic anhydride.

Furthermore, the different initial conformation (switching one of the carbonyl groups into opposite side) of acetic anhydride was also considered to illustrate the effect of fitted charges. The obtained density and viscosity results revealed that no significant changes were observed. The difference between two initial conformer simulation results

is in the range of 0.0001–0.005 g cm^{-3} for density and 0.01–0.05 mPa·s for viscosity, respectively. Therefore, the fitted charges can be used for acetic anhydride pure simulations irrespective of initial conformation.

4. Conclusions

Different charge models such as RESP2, AM1-BCC, CM1 and CM5 were built for acetic anhydride molecule to understand the properties in a bulk phase. The charges, especially RESP2, AM1-BCC and CM5, were fitted based on the obtained electrostatic potential and Hirshfeld population from density functional theory calculations. In the case of RESP2 charges, both gas phase and aqueous phase charges were taken into account in order to include the condensed phase interaction with a typical percentage ratio of 40% gas and 60% aqueous phase. AM1-BCC charges were obtained from ESP of HF/6-31 g(d) method. On the other hand, 1.27 factor was used for CM5 charges, and CM1 charges were extracted from LigParGen server for comparison. These charges were further combined with GAFF/RESP2/AM1-BCC and OPLS /CM1/CM5 potentials to perform the molecular dynamics simulations. The obtained density and viscosity results show that both potentials are in good agreement with experimental values. However, GAFF/RESP2/AM1-BCC potential slightly overestimated the density than OPLS potential. On the other hand, at higher temperature, it was observed that GAFF/RESP2 was more pronounced to experimental values for viscosity prediction; however, GAFF/AM1-BCC predicted the reverse. The calculated radial distribution functions also exhibit similar trend in both cases. Comparing the computational cost for fitting of the investigated charges, AM1-BCC fitting was rapid (about a second in this case) over other methods. Overall, it is stressed that the proposed charges can be combined with GAFF and OPLS potentials and applied to acetic anhydride for bulk phase pure simulation.

Funding

The author gratefully acknowledges the European Commission for funding the InnoRenew project [Grant Agreement # 739574] under the Horizon2020 Widespread-Teaming program, the Republic of Slovenia (investment funding of the Republic of Slovenia and the European Union European Regional Development Fund) and infrastructural ARRS program IO-0035.

CRediT authorship contribution statement

Veerapandian Ponnuchamy: Conceptualization, Validation, Formal analysis, Investigation, Data curation, Writing - original draft, Writing - review & editing, Visualization.

Declaration of Competing Interest

The authors declare that they have no known competing financial interests or personal relationships that could have appeared to influence the work reported in this paper.

Acknowledgement

The author is grateful to Dr. Anna Sandak and Dr. Jakub Sandak for their support and critical reading of the manuscript. This research was carried out using the research facilities of the Wood Modification group at the InnoRenew CoE institute.

References

[1] R.M. Rowell, J.P. Dickerson, Acetylation of Wood, in: Deterioration and Protection of Sustainable Biomaterials, American Chemical Society, 2014, pp. 301–327. https://doi.org/10.1021/bk-2014-1158.ch018.
[2] J. Donald Albright, Leon Goldman, Dimethyl sulfoxide-acid anhydride mixtures for the oxidation of alcohols, J. Am. Chem. Soc. 89 (1967) 2416–2423, https://doi.org/10.1021/ja00986a031.
[3] R.C. Montelaro, R.R. Rueckert, Radiolabeling of proteins and viruses in vitro by acetylation with radioactive acetic anhydride, J. Biol. Chem. 250 (1975) 1413–1421.
[4] J.F. Harper, G. Brooker, Femtomole sensitive radioimmunoassay for cyclic AMP and cyclic GMP after 2'0 acetylation by acetic anhydride in aqueous solution, J. Cyclic Nucleotide Res. 1 (1975) 207–218.
[5] A. Sandak, J. Sandak, M. Brzezicki, A. Kutnar, Bio-based Building Skin, Springer, Singapore, 2019. https://doi.org/10.1007/978-981-13-3747-5.
[6] J. Iqbal, R.R. Srivastava, Cobalt (II) chloride catalyzed acylation of alcohols with acetic anhydride: scope and mechanism, J. Org. Chem. 57 (1992) 2001–2007, https://doi.org/10.1021/jo00033a020.
[7] W.-J. Chun, Y. Koike, H. Ashima, K. Kinoshita, K. Ijima, K. Fujikawa, S. Suzuki, M. Nomura, Y. Iwasawa, K. Asakura, Atomically dispersed Cu species on a TiO2(110) surface precovered with acetic anhydride, Chem. Phys. Lett. 470 (2009) 99–102, https://doi.org/10.1016/j.cplett.2009.01.030.
[8] W.K. Son, J.H. Youk, W.H. Park, Antimicrobial cellulose acetate nanofibers containing silver nanoparticles, Carbohydr. Polym. 65 (2006) 430–434, https://doi.org/10.1016/j.carbpol.2006.01.037.
[9] C.I.K. Diop, H.L. Li, B.J. Xie, J. Shi, Effects of acetic acid/acetic anhydride ratios on the properties of corn starch acetates, Food Chem. 126 (2011) 1662–1669, https://doi.org/10.1016/j.foodchem.2010.12.050.
[10] N. Singh, D. Chawla, J. Singh, Influence of acetic anhydride on physicochemical, morphological and thermal properties of corn and potato starch, Food Chem. 86 (2004) 601–608, https://doi.org/10.1016/j.foodchem.2003.10.008.
[11] S. Fischer, K. Thümmler, B. Volkert, K. Hettrich, I. Schmidt, K. Fischer, Properties and applications of cellulose acetate, Macromolecular Symposia 262 (2008) 89–96, https://doi.org/10.1002/masy.200850210.
[12] L.N. Silva, V.L.C. Gonçalves, C.J.A. Mota, Catalytic acetylation of glycerol with acetic anhydride, Catal. Commun. 11 (2010) 1036–1039, https://doi.org/10.1016/j.catcom.2010.05.007.
[13] R. Fujisawa, T. Ohno, J.F. Kaneyasu, P. Leproux, V. Couderc, H. Kita, H. Kano, Dynamical study of the water penetration process into a cellulose acetate film studied by coherent anti-Stokes Raman scattering (CARS) microspectroscopy, Chem. Phys. Lett. 655–656 (2016) 86–90, https://doi.org/10.1016/j.cplett.2016.05.038.
[14] J.K. Cunningham, L.-M. Liu, R.C. Callaghan, Essential ("Precursor") chemical control for heroin: impact of acetic anhydride regulation on US heroin availability, Drug Alcohol Dependence 133 (2013) 520–528, https://doi.org/10.1016/j.drugalcdep.2013.07.014.
[15] James Revill, Strategic governance of IEDs, in: James Revill (Ed.), Improvised Explosive Devices, Springer International Publishing, Cham, 2016, pp. 91–109, , https://doi.org/10.1007/978-3-319-33834-7_6.
[16] L.R. Odell, J. Skopec, A. McCluskey, A 'cold synthesis' of heroin and implications in heroin signature analysis: utility of trifluoroacetic/acetic anhydride in the acetylation of morphine, Forensic Sci. Int. 164 (2006) 221–229, https://doi.org/10.1016/j.forsciint.2006.02.009.
[17] Junmei Wang, Romain M. Wolf, James W. Caldwell, Peter A. Kollman, David A. Case, Development and testing of a general amber force field, J. Comput. Chem. 25 (9) (2004) 1157–1174, https://doi.org/10.1002/(ISSN)1096-987X10.1002/jcc.v25:910.1002/jcc.20035.
[18] W.L. Jorgensen, D.S. Maxwell, J. Tirado-Rives, Development and testing of the OPLS all-atom force field on conformational energetics and properties of organic liquids, J. Am. Chem. Soc. 118 (1996) 11225–11236, https://doi.org/10.1021/ja9621760.
[19] C.I. Bayly, P. Cieplak, W. Cornell, P.A. Kollman, A well-behaved electrostatic potential based method using charge restraints for deriving atomic charges: the RESP model, J. Phys. Chem. 97 (1993) 10269–10280, https://doi.org/10.1021/j100142a004.
[20] A. Jakalian, B.L. Bush, D.B. Jack, C.I. Bayly, Fast, efficient generation of high-quality atomic charges. AM1-BCC model: I. Method, J. Comput. Chem. 21 (2000) 132–146, https://doi.org/10.1002/(SICI)1096-987X(20000130)21:2<132:: AID-JCC5>3.0.CO;2-P.
[21] A. Jakalian, D.B. Jack, C.I. Bayly, Fast, efficient generation of high-quality atomic charges. AM1-BCC model: II. Parameterization and validation, J. Comput. Chem. 23 (2002) 1623–1641, https://doi.org/10.1002/jcc.10128.
[22] D.S. Cerutti, J.E. Rice, W.C. Swope, D.A. Case, Derivation of fixed partial charges for amino acids accommodating a specific water model and implicit polarization, J. Phys. Chem. B 117 (2013) 2328–2338, https://doi.org/10.1021/jp311851r.
[23] J.Z. Vilseck, J. Tirado-Rives, W.L. Jorgensen, Evaluation of CM5 charges for condensed-phase modeling, J. Chem. Theory Comput. 10 (2014) 2802–2812, https://doi.org/10.1021/ct500016d.
[24] L.S. Dodda, J.Z. Vilseck, J. Tirado-Rives, W.L. Jorgensen, 1.14*CM1A-LBCC: localized bond-charge corrected CM1A charges for condensed-phase simulations, J. Phys. Chem. B 121 (2017) 3864–3870, https://doi.org/10.1021/acs.jpcb.7b00272.
[25] C.M. Breneman, K.B. Wiberg, Determining atom-centered monopoles from molecular electrostatic potentials. The need for high sampling density in formamide conformational analysis, J. Comput. Chem. 11 (1990) 361–373, https://doi.org/10.1002/jcc.540110311.
[26] M. Udier-Blagović, P.M.D. Tirado, S.A. Pearlman, W.L. Jorgensen, Accuracy of free energies of hydration using CM1 and CM3 atomic charges, J. Comput. Chem. 25 (2004) 1322–1332, https://doi.org/10.1002/jcc.20059.
[27] M. Schauperl, P.S. Nerenberg, H. Jang, L.-P. Wang, C.I. Bayly, D.L. Mobley, M.K. Gilson, Non-bonded force field model with advanced restrained electrostatic potential charges (RESP2), Commun. Chem. 3 (2020) 1–11, https://doi.org/10.

1038/s42004-020-0291-4.
[28] A.V. Marenich, S.V. Jerome, C.J. Cramer, D.G. Truhlar, Charge model 5: an extension of hirshfeld population analysis for the accurate description of molecular interactions in gaseous and condensed phases, J. Chem. Theory Comput. 8 (2012) 527–541, https://doi.org/10.1021/ct200866d.
[29] F.L. Hirshfeld, Bonded-atom fragments for describing molecular charge densities, Theor. Chim. Acta 44 (1977) 129–138, https://doi.org/10.1007/BF00549096.
[30] M.W. Schmidt, K.K. Baldridge, J.A. Boatz, S.T. Elbert, M.S. Gordon, J.H. Jensen, S. Koseki, N. Matsunaga, K.A. Nguyen, S. Su, T.L. Windus, M. Dupuis, J.A. Montgomery, General atomic and molecular electronic structure system, J. Comput. Chem. 14 (1993) 1347–1363, https://doi.org/10.1002/jcc.540141112.
[31] V.N. Staroverov, G.E. Scuseria, J. Tao, J.P. Perdew, Comparative assessment of a new nonempirical density functional: molecules and hydrogen-bonded complexes, J. Chem. Phys. 119 (2003) 12129–12137, https://doi.org/10.1063/1.1626543.
[32] B.P. Pritchard, D. Altarawy, B. Didier, T.D. Gibson, T.L. Windus, New basis set exchange: an open, up-to-date resource for the molecular sciences community, J. Chem. Inf. Model. 59 (2019) 4814–4820, https://doi.org/10.1021/acs.jcim.9b00725.
[33] P. Bleiziffer, K. Schaller, S. Riniker, Machine learning of partial charges derived from high-quality quantum-mechanical calculations, J. Chem. Inf. Model. 58 (2018) 579–590, https://doi.org/10.1021/acs.jcim.7b00663.
[34] G. Schaftenaar, J.H. Noordik, Molden: a pre- and post-processing program for molecular and electronic structures*, J. Comput. Aided Mol. Des. 14 (2000) 123–134, https://doi.org/10.1023/A:1008193805436.
[35] U.C. Singh, P.A. Kollman, An approach to computing electrostatic charges for molecules, J. Comput. Chem. 5 (1984) 129–145, https://doi.org/10.1002/jcc.540050204.
[36] T. Lu, F. Chen, Multiwfn: a multifunctional wavefunction analyzer, J. Comput. Chem. 33 (2012) 580–592, https://doi.org/10.1002/jcc.22885.
[37] J. Wang, W. Wang, P.A. Kollman, D.A. Case, Automatic atom type and bond type perception in molecular mechanical calculations, J. Mol. Graph. Model. 25 (2006) 247–260, https://doi.org/10.1016/j.jmgm.2005.12.005.
[38] The MG3S basis is available at the following website: http://comp.chem.umn.edu/basissets/basis.cgi (accessed April 29, 2020).
[39] S. Plimpton, Fast parallel algorithms for short-range molecular dynamics, J. Comput. Phys. 117 (1995) 1–19, https://doi.org/10.1006/jcph.1995.1039.
[40] L.S. Dodda, I. Cabeza de Vaca, J. Tirado-Rives, W.L. Jorgensen, LigParGen web server: an automatic OPLS-AA parameter generator for organic ligands, Nucleic Acids Res. 45 (2017) W331–W336, https://doi.org/10.1093/nar/gkx312.
[41] L. Martínez, R. Andrade, E.G. Birgin, J.M. Martínez, PACKMOL: a package for building initial configurations for molecular dynamics simulations, J. Comput. Chem. 30 (2009) 2157–2164, https://doi.org/10.1002/jcc.21224.
[42] M.P. Allen, D.J. Tildesley, Computer Simulation of Liquids, Oxford University Press, 2017.
[43] L. Dai, D. He, M. Lei, Y. Chen, Densities and viscosities of binary mixtures of acetic acid with acetic anhydride and methenamine at different temperatures, J. Chem. Eng. Data 53 (2008) 2892–2896, https://doi.org/10.1021/je8003782.
[44] C. Caleman, P.J. van Maaren, M. Hong, J.S. Hub, L.T. Costa, D. van der Spoel, Force field benchmark of organic liquids: density, enthalpy of vaporization, heat capacities, surface tension, isothermal compressibility, volumetric expansion coefficient, and dielectric constant, J. Chem. Theory Comput. 8 (2012) 61–74, https://doi.org/10.1021/ct200731v.